Phoenix: International Multidisciplinary Research Journal
Vol 4, No. 2, April-June, 2026
ISSN: 2583-6897

SYNTHESIS NOVEL SCHIFF BASE AND ITS TRANSITION METAL COMPLEXES: CHARACTERIZATION AND STUDY OF ITS BIOLOGICAL ACTIVITY.

Kapil Totawar
Department of Chemistry NES Science College, Nanded (MS)
L. P. Shinde
Department of Chemistry NES Science College, Nanded (MS)
Anil Shinde*
MJPV Arts, Commerce And Shri VKK Science College Dhadagon (MS)

ABSTRACT: Schiff bases, which are flexible ligands, are created when primary amines with carbonyl groups condense. These substances are very important in the fields of pharmacology and medicine due to their wide range of biological action. Most of them have biological characteristics such as antifungal, antibacterial, and anticancer activity. Transition metal complexes with biological activity that are produced from Schiff base ligands have been the subject of numerous investigations. This summarizes the biological activity and synthesis of Schiff bases and related transition complexes.

Keywords: Schiff bases, metal complexes, antibacterial activity, anticancer activity, and nonlinear optical properties

Introduction

In recent years, metal chelates have harvested significant attention due to their diverse properties and widespread applications across biology and chemistry[1-7]. While numerous organic substances exhibit biological activities, their potency often undergoes substantial changes when complexed with metals[8-9]. Moreover, the formation of metal chelates has significantly enhanced their utility in analytical, catalytic, pharmaceutical, industrial, and other fields[10-12]. While a variety of complexing and chelating ligands exist, the donor atoms that coordinate with metal ions are primarily limited to strongly non-metallic elements like nitrogen, oxygen, sulfur or phosphorus. Common electron donor groups include carboxylic (-COOH), phenolic (-OH), thio (-SH), oxime (=N-OH), and imine (=NH) groups, which liberate protons upon complexation. Although achieving absolute specificity in a chelating agent remains a challenging endeavor, considerable research has been dedicated to this goal. As our understanding of donor and central atoms continues to evolve, more selective and sensitive reagents are continually being developed. Amongst these promising agents, Schiff bases have begun as a particularly vital class of compounds.

Schiff bases, named after their discoverer Hugo Schiff, are formed when primary amines react with carbonyl compounds [13]. These compounds typically have the structure RC=NR', where R and R' can be various alkyl, cyclohexyl, aryl or heterocyclic groups, possibly with different substituents.

Schiff bases are effective chelating agents when they contain, in addition to the

azomethine nitrogen (>C=N-), a supplementary ligating group like -OH, -SH, -NO_2, or -NH_2. This allows for the formation of six-membered chelate rings upon complexation with a metal ion. Chelating ligands with O and N donor atoms are particularly interesting due to their diverse biological activities and the various bonding modes they exhibit with metal ions. Numerous Schiff base complexes have demonstrated promising properties in areas such as anti-inflammation, antipyretic effects, analgesia, antidiabetic treatment, antibacterial activity, anticancer therapy, and HIV prevention. Azomethine derivatives and their transition metal complexes have. shown notable prospective in inhibiting the growth of several pathogenic microorganisms [14].

Present work deals with the preparation of Schiff base ligand namely 2-(4-(trifluoromethyl)phenyl)imino)methyl)phenol (abbreviated as TFPMP-SB3) by condensation of 4-(trifluoromethyl)benzenamine and 2-hydroxy benzaldehyde (Salicydehyde). The Schiff base ligand is then condensed with various metal salts to give respective metal complexes. The characterization of these compounds were carried out by physical parameters and spectral analysis namely colour, melting point, ^{1}HNMR, IR, UV, Magnetic measurements, ESR, XRD and TGA studies. The spectral analyses are used for elucidating the structure of ligand and metal complexes. Biological activity of the compounds has been studied for Gram positive bacterial strains of Bacillus subtillis and Staphylococcus aureus Gram negative bacterial strains of Escherichia coli and Klebsiella pneumonia.

Materials and Methods:

Chemicals:

The chemicals used in this study included salicylaldehyde (Merck, AR grade), ethanol (Merck, ARgrade), cobalt(II) chloride dihydrate (Sigma Aldrich), nickel(II) chloride hexahydrate (Sigma Aldrich), copper(II) chloride dihydrate (Sigma Aldrich), and manganese(II) chloride tetrahydrate (Sigma Aldrich).

Apparatus:

Borosilicate glassware was used throughout the experiments. An analytical balance with a sensitivity of 0.1 mg was employed for weighing samples exceeding 50 mg. For samples weighing less than 50 mg, a semi-micro balance was utilized.

The Schiff base ligand, 2-(4-(trifluoromethyl)phenyl)imino)methyl)phenol (Fig 4.1), was prepared by the equimolar condensation of 4-(trifluoromethyl) benzenamine with salicyldehyde (2-Hydroxy benzaldehyde). Briefly, salicyldehyde (0.01 mole) in 10 mL of ethanol was added to a stirred ethanolic solution (10 mL) of the amine (0.01 mole). The resulting mixture was refluxed for 2-3 hours. Upon cooling, a precipitate formed immediately. This precipitate was then collected by filtration, washed with ethanol, and subsequently dried. Recrystallization of the crude product from aqueous ethanol afforded the pure product in 85% yield. The synthetic route for the Schiff base is depicted in Figure 1.1.

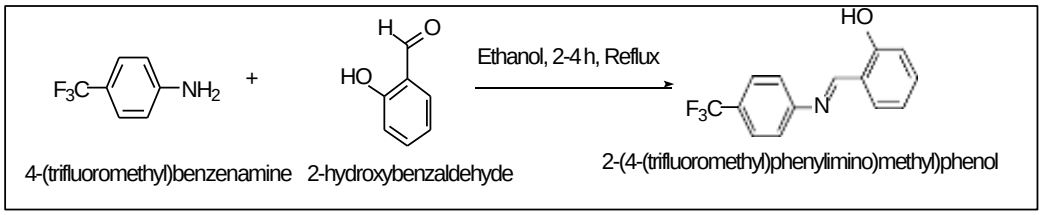

Fig 4.1: Preparation of Ligand (TFPMP-SB3)

Equimolar solutions of the ligand and the respective metal chloride salts (Ni(II), Cu(II), Co(II) and Mn(II)) were prepared in ethanol at a 2:1 ligand-to-metal molar ratio. These mixtures were then heated in a water bath for 2-3 hrs. Following heating, the reaction mixtures were cooled, resulting in the precipitation of colored solids. These solids were subsequently collected by filtration, thoroughly washed with ethanol to remove any unreacted starting materials, and then dried under vacuum. This general synthetic procedure was consistently used for all the metal complexes.

Characterization of the Schiff base ligand and its metal complexes involved various spectroscopic and analytical techniques, including UV-Visible, PMR, IR, XRD, ESR, magnetic susceptibility measurements, and TGA. The elemental analysis (C, H, N) of the compounds was carried out on a Perkin Elmer 240 C (USA) elemental analyzer, Melting points of compounds were done with open glass capillary tubes on a Polmon instrument (model No. MP-96). NMR spectra of all the prepared ligands were recorded in $CDCl_3$ / Deuterated DMSO using TMS as an internal standard reference on a Bruker 400 MHz spectrometer. Vibrational Infrared spectra of the ligand and the metal complexes were recorded in the range of 4000-400 cm^{-1} using a Shimadzu IRPrestige-21 spectrophotometer from KBr discs. Electronic spectra of the complexes were recorded on a Shimadzu UV-Vis 2600 spectrophotometer in the wavelength range of 200-800 nm using DMSO as solvent. The thermo gravimetric analysis was carried out in dynamic nitrogen atmosphere with a heating rate of 10^oC min^{-1} using Mettler Toledo Star system in the temperature range of 30-1000^oC. EPR spectra of the Cu (II) complexes were recorded using JES-FA 200 ESR spectrometer (JEOL-Japan) at liquid nitrogen temperature (77K).

I. Physical Parameters:

The Schiff base described herein represents a novel compound, synthesized for the first time via a condensation reaction between the corresponding amine and aldehyde, yielding a crystalline solid. The resulting transition metal complexes exhibit distinct bright colors and are non-hygroscopic. These complexes demonstrate insolubility in water but exhibit complete solubility in DMSO at ambient temperature. Furthermore, all synthesized metal complexes demonstrate significant thermal stability. Comprehensive physical parameters and spectral data for both the ligand and the synthesized metal complexes are detailed in the tables presented below table.1.1.

S.No	Compound	Color	Yield (%)	MP
1	TFPMP-SB3	Off white	83	174
2	$(TFPMP\text{-}SB3)_2Cu$	Cream	78	260
3	$(TFPMP\text{-}SB3)_2$ Ni	buff	76	276
4	$(TFPMP\text{-}SB3)_2$ Co	Pale green	80	295
5	$(TFPMP\text{-}SB3)_2(H_2O)_2Mn$	Brown	74	280

Table.1.1: Colour, Yeild and Melting points of (TFPMP-SB3) and its Metal Complexes.

II. Elemental Analysis of TFPMP-SB3 and its metal Complexes

S. No	Compound	Molecular formula	Mw	Elemental analysis Observed (Calculated)			
				% C	% H	% N	% M
1	TFPMP-SB3	$C_{14}H_{10}F_3NO$	265.07	63.66 (63.40)	4.00 (3.80)	5.48 (5.28)	
2	$(TFPMP\text{-}SB3)_2$ Cu	$C_{28}H_{18}CuF_6N_2O_2$	591.06	56.81 (57.01)	3.06 (3.24)	4.73 (4.91)	10.73 (10.95)
3	$(TFPMP\text{-}SB3)_2Ni$	$C_{28}H_{18}NiF_6N_2C_2$	586.06	57.28 (57.49)	3.09 (58.31)	4.77 (4.44)	10.00 (10.22)
4	$(TFPMP\text{-}SB3)_2$ Co	$C_{28}H_{18}CoF_6N_2O_2$	587.06	57.25 (57.46)	3.09 (3.12)	4.77 (5.99)	10.03 (10.23)
5	$(TFPMP\text{-}SB3)_2(H_2O)_2$ Mn	$C_{28}H_{18}F_6MnN_2O_2$	583.07	57.65 (57.85)	3.11 (3.22)	4.80 (5.01)	9.42 (9.63)

Table 1.2: Elemental Analysis of (TFPMP-SB3) and its Metal Complexes.

III. Electronic Absorption spectra:

The UV-Visible absorption spectra of synthesized ligand and its metal complexes were recorded in DMSO solution at room temperature in 200-800 nm range and the data are presented in table 4.3.The spectra of TFPMP-SB3 and its all complexes are shown in Figure 1.2 to Figure 1.6. The electronic spectral data of the complexes with all the ligands are presented in table 1.3.

The intense band in the UV region at 260 nm for complex copper, 277 nm for nickel complex, 265 nm for cobalt complex, 208 for Manganese complexis attributed to intra-ligand benzene ring π-π* transition. Another intense band at 442nm for copper complex, 326 and 435 nm for Ni complex, 380nm for cobalt complex and 355 for Manganese complex is due to the azomethine chromophore n-π* transition of coordinated Schiff base ligands.

Furthermore, Cu (II) metal complexes also showed d-d band in the visible region at 538 nm range. This band certainly due to the d-d transition ($^2B_{1g} \rightarrow {}^2E_g$)[15-18]. Actually, in square planar complexes, three transitions are possible but due to overlapping of these bands result in a single broad band. For nickel(II) complexes, two absorption bands in the range at 435 and 526 nm. These bands are attributed to nickel(II) square planar complex corresponding to $^1A_{1g}$-$^1A_{2g}$ and $^1A_{1g}$-$^1B_{1g}$ transitions respectively. For square planar complexes three transitions are expected but $^1A_{1g}$-$^1E_{1g}$ transition is masked by charge transfer (CT) (326 nm) band[19]. The Cobalt (II) metal complexes also showed d-d band in the visible region at 552 nm. This band certainly due to the d-d transition ($^1A_{1g} \rightarrow {}^1B_{1g}$)[6-7].The Mn complex displayed a λ_{max} at 355 nm, which could be attributed to a charge transfer transition. A distinct ligand-to-metal charge transfer (LMCT) band was observed at 546 nm. As expected for Mn (II) complexes, d-d transitions, being both spin-forbidden and Laporte-forbidden, were not observed in the electronic spectrum. These transitions typically possess such low intensity that they are effectively undetectable [20-21].

S.No	Compound	Transitions in nm
1	TFPMP-SB3	256 and 308
2	$(TFPMP\text{-}SB3)_2Cu$	260, 442 and 538
3	$(TFPMP\text{-}SB3)_2Ni$	277, 326, 435 and 526
4	$(TFPMP\text{-}SB3)_2Co$	265, 380 and 552
5	$(TFPMP\text{-}SB3)_2\ (H_2O)_2Mn$	208, 355 and 546

Table1.3: Electronic absorption spectra values for (TFPMP-SB3) and its metal complexes.

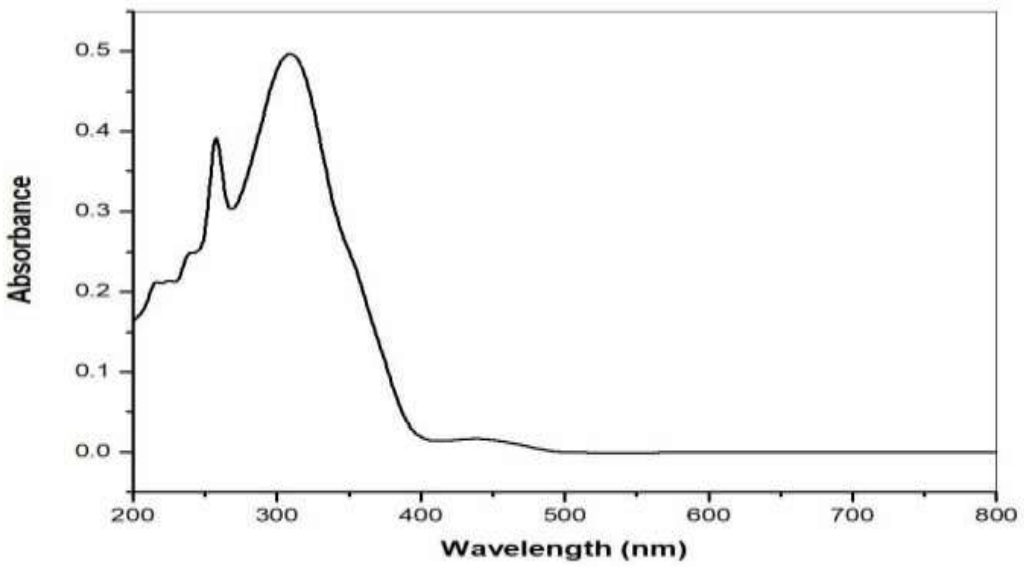

Fig 1.2: UV-Visible spectrum of (TFPMP-SB3)

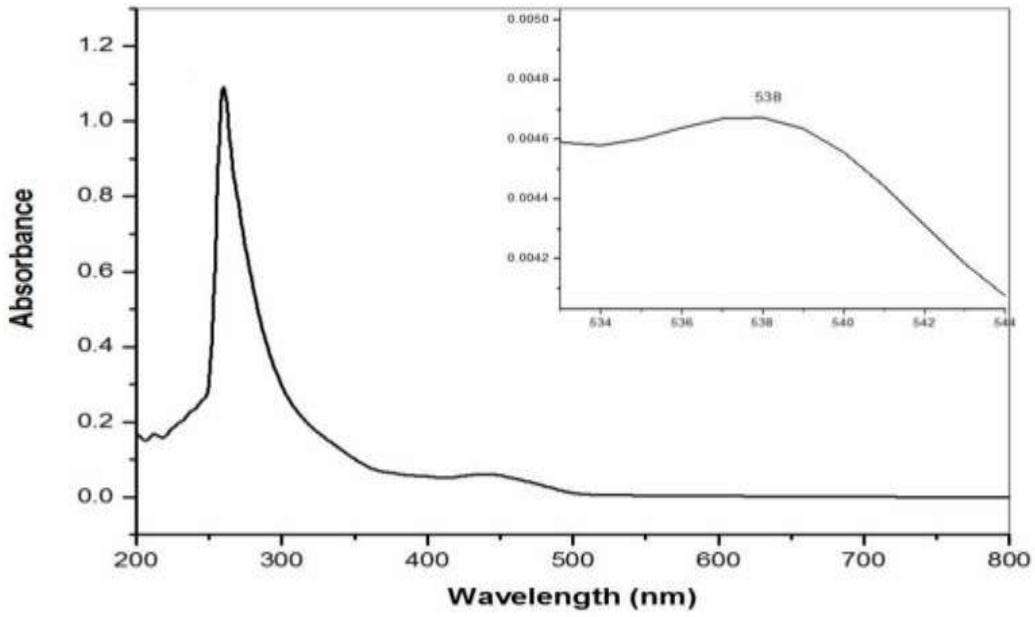

Fig 1.3: UV-Visible spectrum of complex $(TFPMP\text{-}SB3)_2Cu$

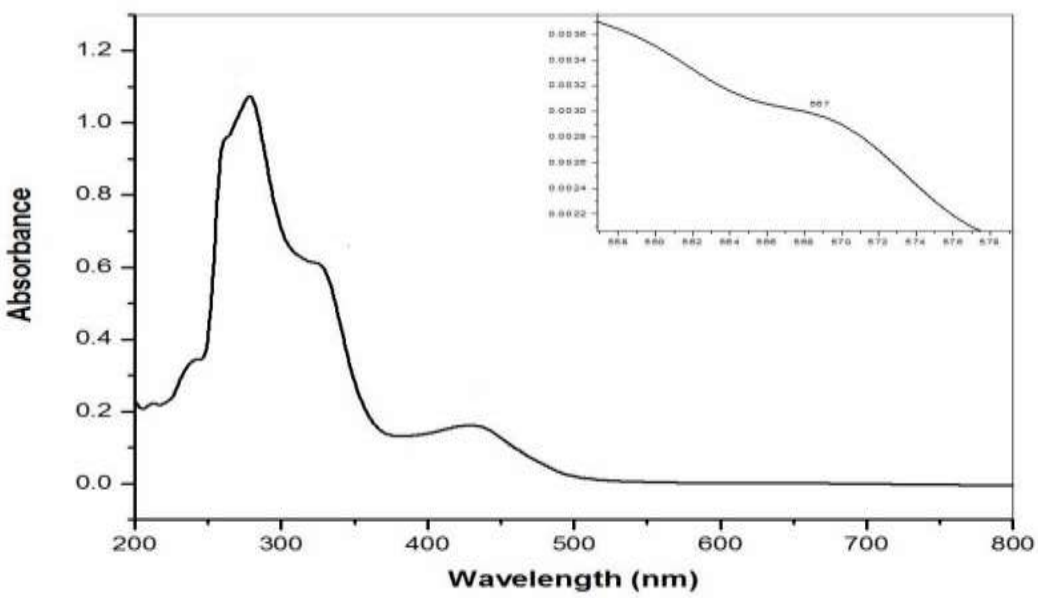

Fig 1.4: UV-Visible spectrum of complex $(TFPMP\text{-}SB3)_2Ni$

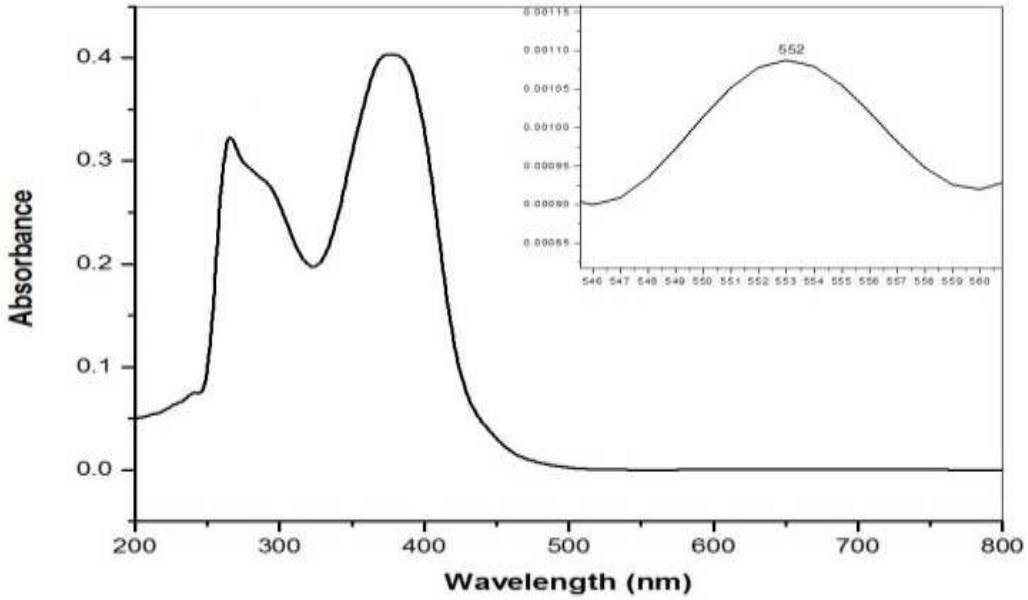

Fig 1.5: UV-Visible spectrum of complex $(TFPMP\text{-}SB3)_2Co$

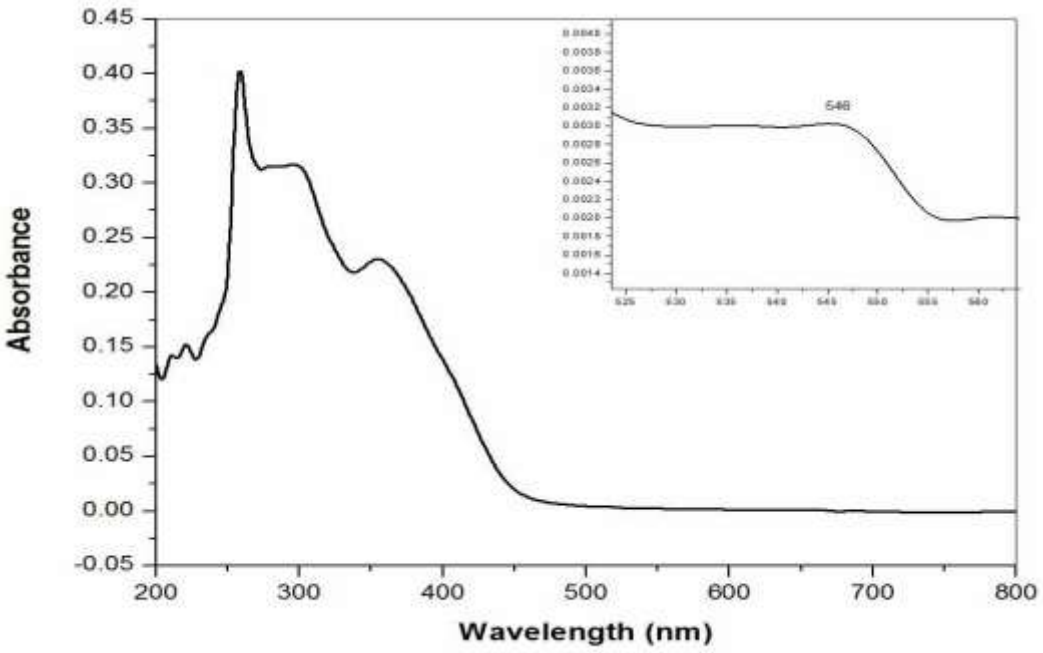

Fig 1.6: UV-Visible spectrum of complex $(TFPMP\text{-}SB3)_2(H_2O)_2Mn$

IV. IR spectra

The FT-IR spectra of the Schiff base TFPMP-SB3 and its corresponding metal complexes, recorded within the 5000-400 cm^{-1} range using KBr discs (as detailed in Table 1.4) exhibit complex profiles characterized by a multitude of bands with varying intensities. Due to this complexity, a complete and unambiguous assignment of all observed bands is challenging. However, based on comparisons with previously reported data in the literature, it is possible to identify and assign some key bands corresponding to important functional groups present in the Schiff base and its complexes.

The Schiff base (TFPMP-SB3) displays a characteristic C=N stretching vibration at 1626 cm^{-1}, indicative of the azomethine function. Upon complexation with metals, this vibration shifts to a lower frequency range of 1598-1609 cm^{-1}. This significant shift in the νC=N stretching frequency of the extra nuclear C=N linkage strongly suggests the involvement of the azomethine nitrogen in coordination to the metal center. Consequently, the observed bands within the 1598-1609cm^{-1} region serve as confirmation of the presence and coordination of the C=N linkage within the resulting metal complexes.

The FT-IR spectra of the metal complexes of the Schiff base exhibit medium to weak intensity bands in the 415-436 cm^{-1} and 495-515 cm^{-1} regions. These bands are attributed to M-N and M-O stretching vibrations, respectively[22-23]. This confirms that the metal is bonded to the Schiff base through both the azomethine nitrogen and the oxygen atom of the deprotonated OH group.

S.No	Compound	ν (O-H)	ν (H_2O)	ν (CH=N)	ν(C-O	ν (M-O)	ν(M-N)
1	TFPMP-SB3	3430	-	1626	1160	-	-
2	$(TFPMP\text{-}SB3)_2$ Cu	-	-	1609	1183	515	426
3	$(TFPMP\text{-}SB3)_2$ Ni	-	-	1603	1172	502	436
4	$(TFPMP\text{-}SB3)_2$ Co	-	-	1598	1170	503	415
5	$(TFPMP\text{-}SB3)_2(H_2O)_2Mn$	-	3395	1604	1178	495	425

Table 1.4: IR Spectral values of Schiff base and metal complexes

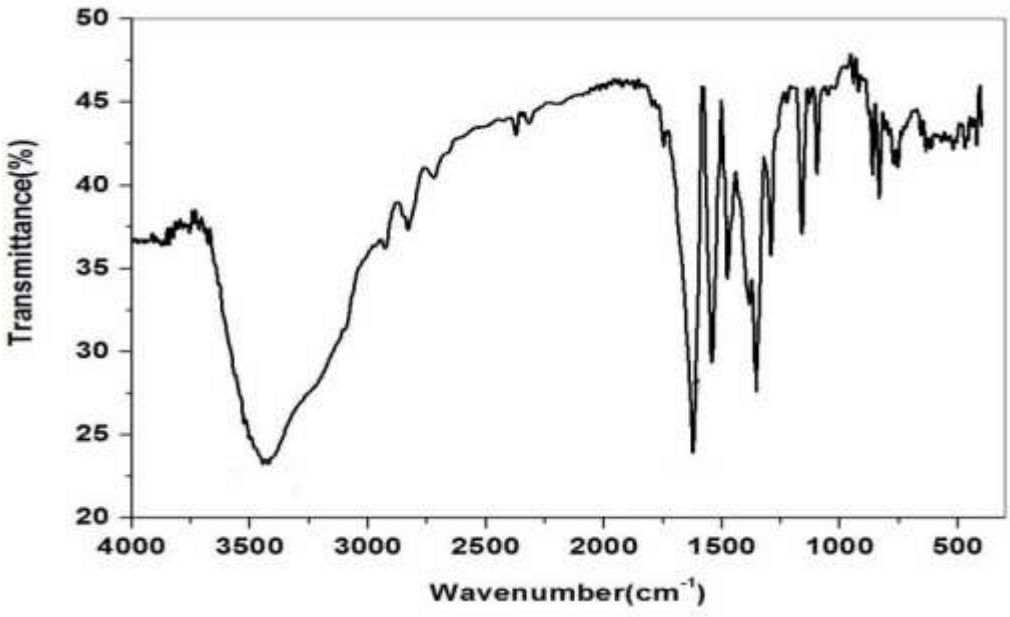

Fig 1.7: IR Spectrum of ligand

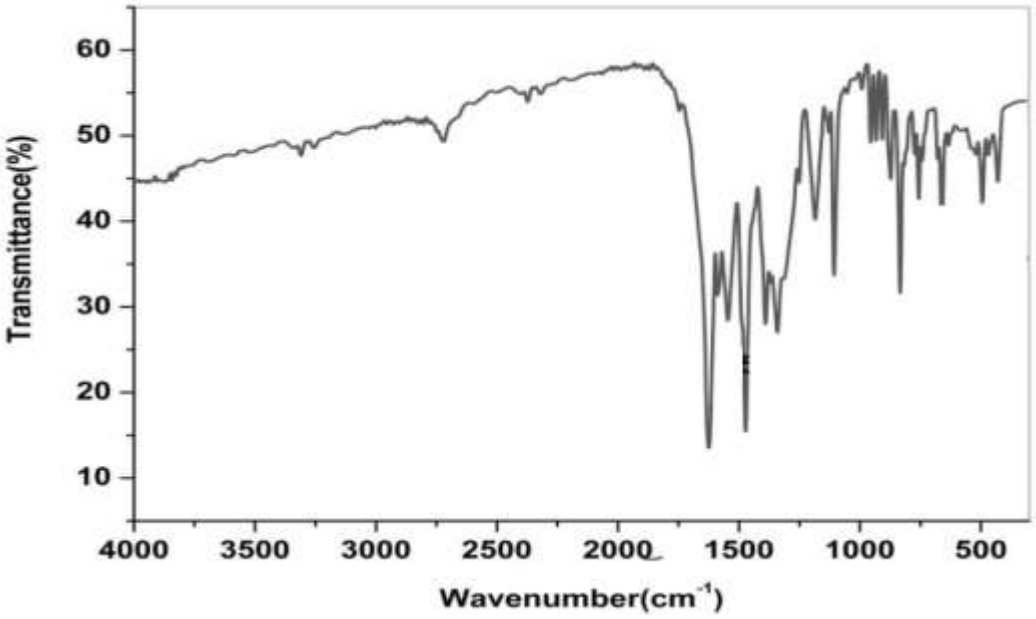

Fig 1.8: IR Spectrum of complex $(TFPMP\text{-}SB3)_2Cu$

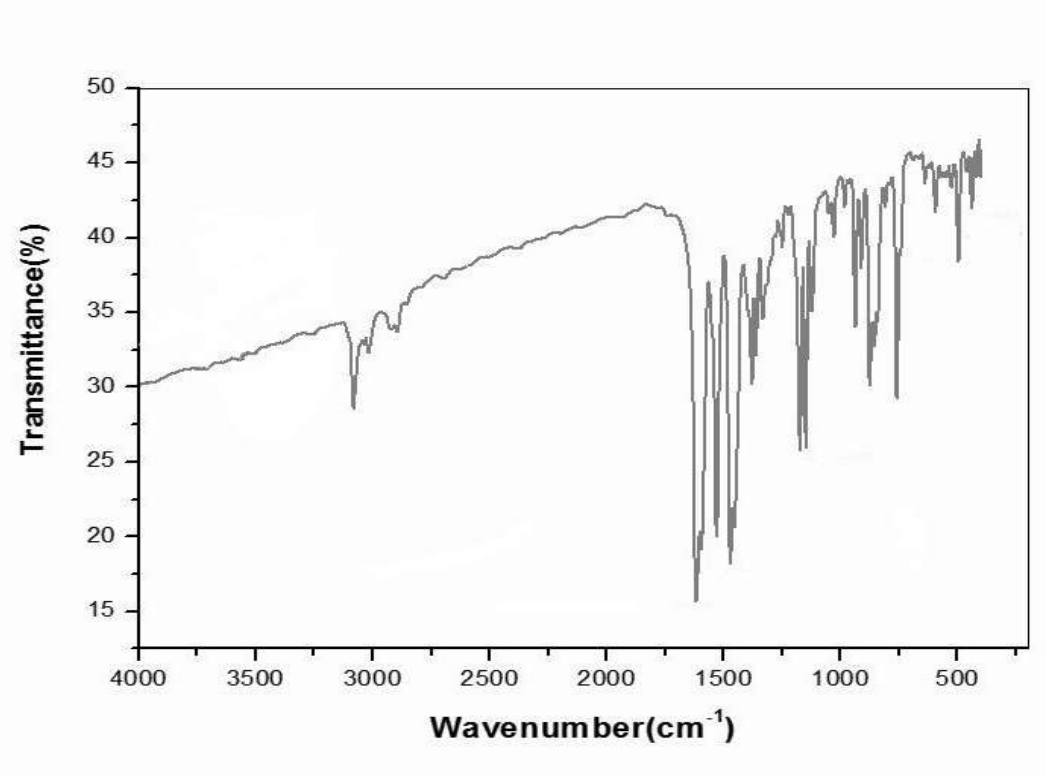

Fig 1.9: IR Spectrum of complex $(TFPMP\text{-}SB3)_2Ni$

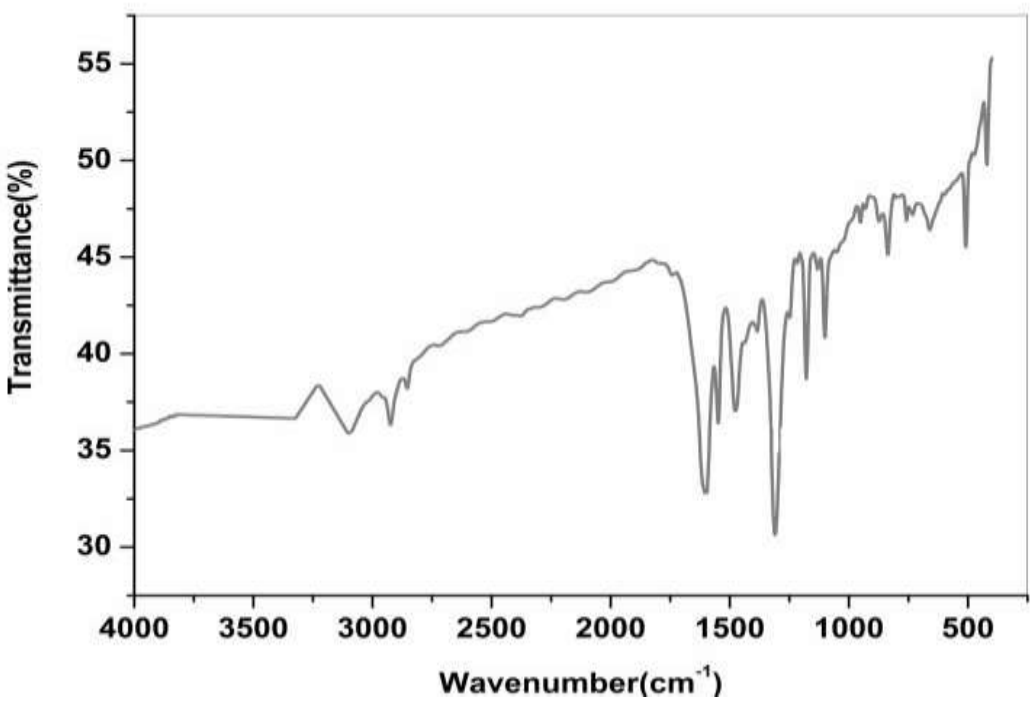

Fig 1.10: IR Spectrum of complex $(TFPMP\text{-}SB3)_2Co$

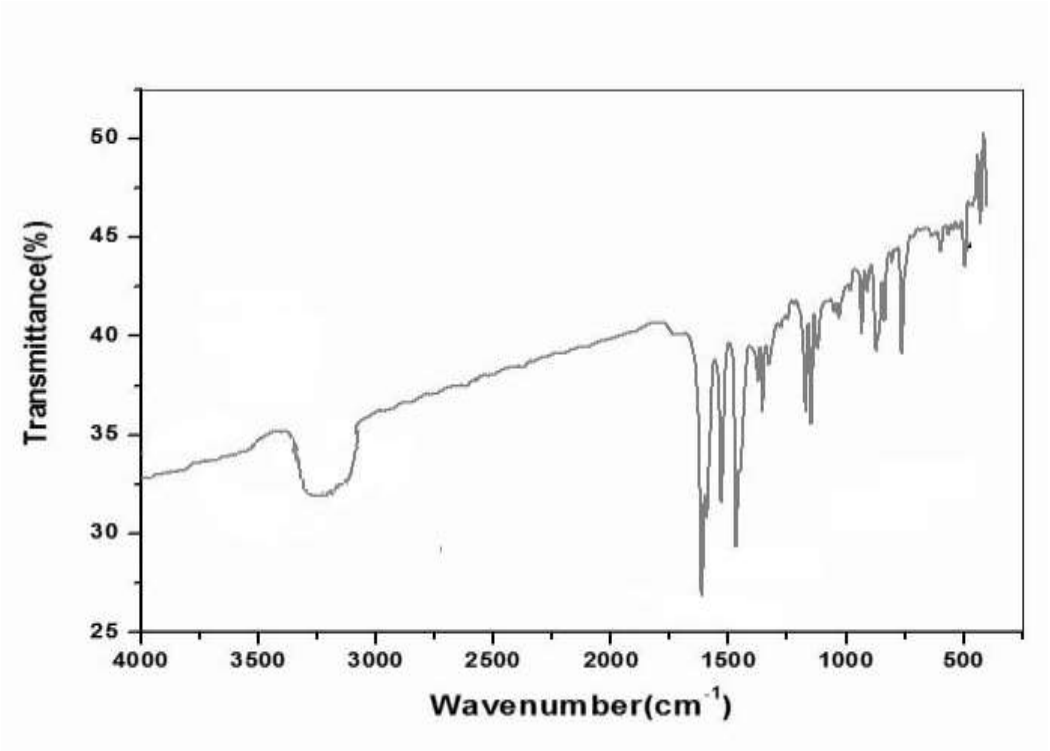

Fig 1.11: IR Spectrum of complex $(TFPMP\text{-}SB3)_2(H_2O)_2Mn$

V. Thermal analysis

Thermal analysis (TGA/DTA) of the complexes, illustrated in Figures 1.12-1.14, reveals a two-step decomposition process occurring between 280°C and 855°C. The initial decomposition step, observed in the 280-457°C range, is attributed to the loss of the starting ligand moiety. The second step, occurring between 440°C and 855°C, corresponds to the complete removal of the organic component of the ligand, leaving behind a metal oxide residue. The observed weight loss is further corroborated by endothermic bands present in the corresponding DTA curves, aligning with the temperature regions where weight loss is observed in the TGA curves.Manganese complex an initial weight loss was observed between 110°C and 200°C, consistent with the elimination of coordinated water molecules, suggesting the presence of such water molecules within the complex structure. A gradual, continued mass loss was observed up to 300°C, likely due to the decomposition and loss of volatile components or ligands. Beyond this temperature, a plateau region was reached in the TGA curve, indicative of the formation of a stable metal oxide residue.

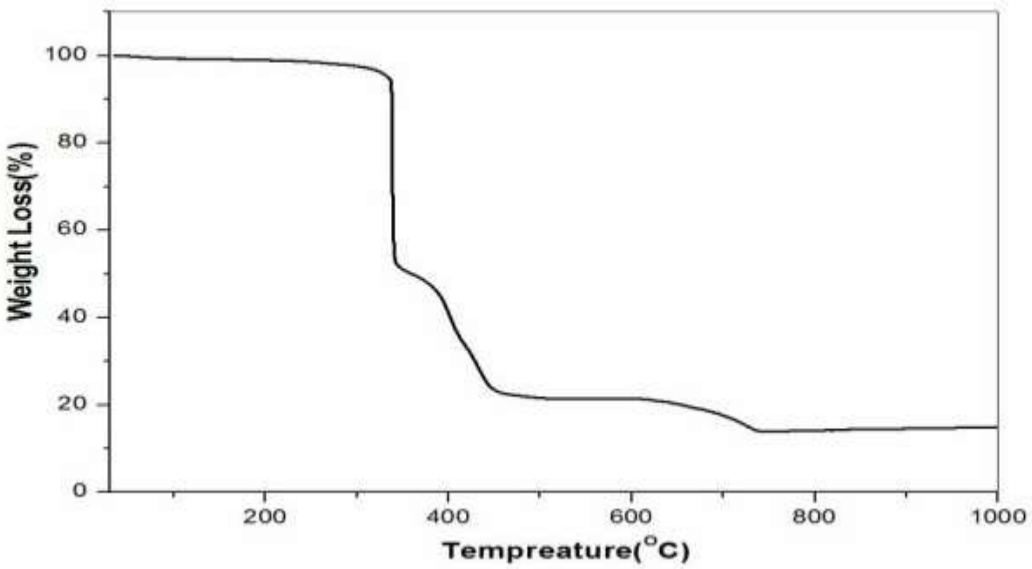

Fig 1.12: TGA & DTA of $(TFPMP\text{-}SB3)_2Cu$

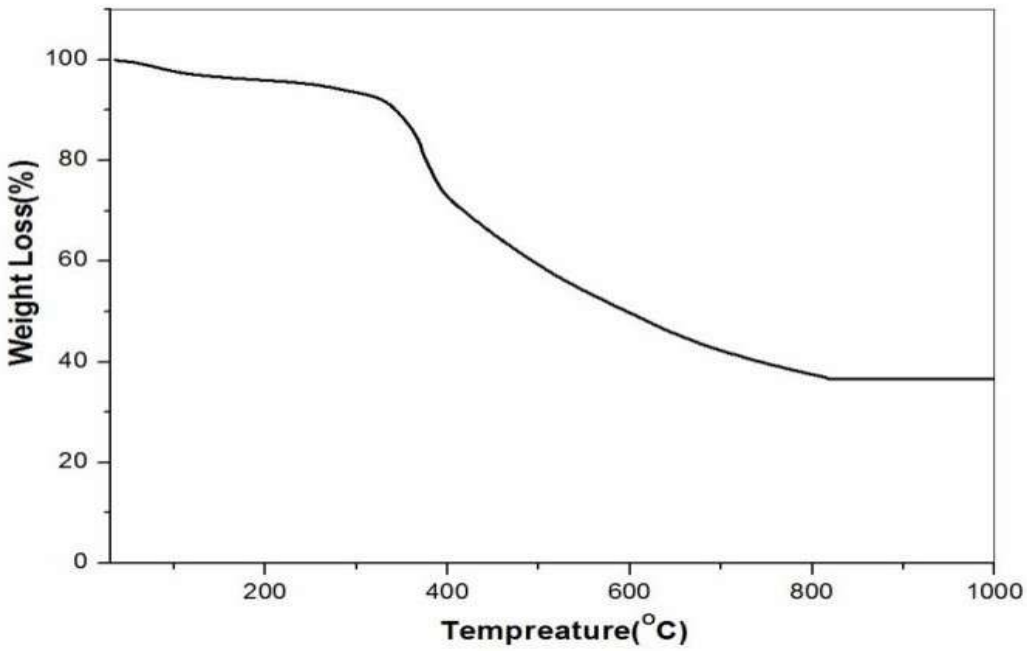

Fig 1.13: TGA & DTA of $(TFPMP\text{-}SB3)_2Ni$

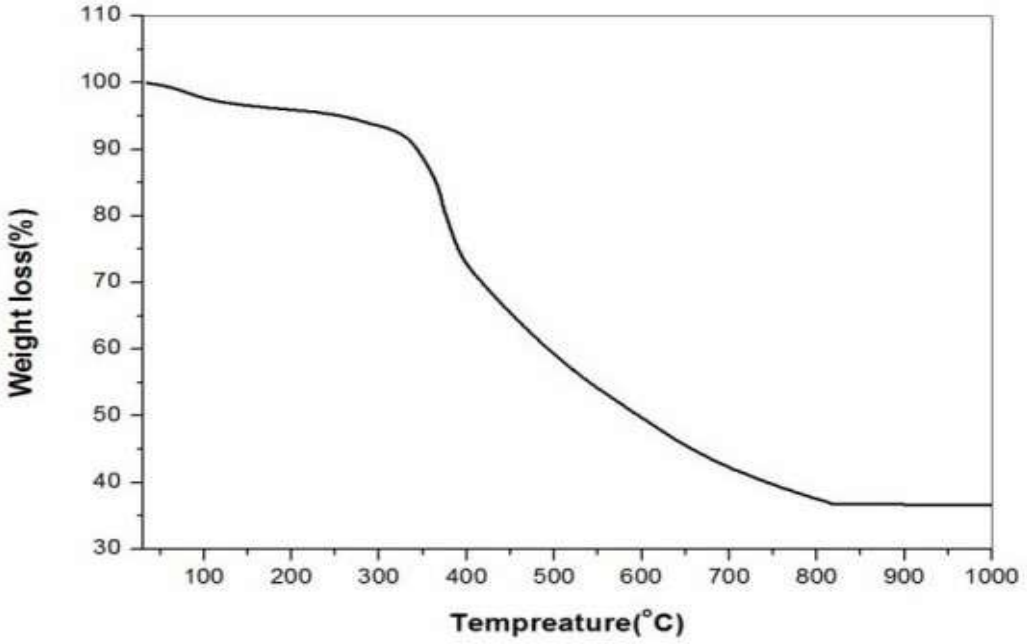

Fig 1.14: TG & DTA analysis spectrum of $(TFPMP\text{-}SB3)_2Co$

VI. Magnetic moments:

According to Figgis, the magnetic moment values of copper (II) complexes can be indicative of their geometry. He proposed that tetrahedral copper (II) complexes would exhibit magnetic moments exceeding 1.97 B.M, whereas those with square planar and distorted octahedral geometries would have values below this threshold. This distinction arises from the expectation of orbital contribution in the former case and its absence in the latter due to a non-degenerate ground state. Furthermore, square planar and tetragonal complexes generally display magnetic moments slightly higher than the spin-only value of 1.73 B.M, a phenomenon attributed to spin-orbit coupling.

The magnetic moments of the copper (II) complex measured in this study at room temperature were found to be slightly higher than the spin-only value, ranging from 1.73 B.M. This observation is indicative of a square planar geometry with one unpaired electron. The small increase in the magnetic moment beyond the spin-only value can be attributed to spin-orbit coupling. Combining the magnetic moment data with electronic spectral and analytical data provides strong evidence for a square planar geometry in the copper (II) complex examined.

The magnetic activity of nickel (II) complex is influenced by their geometry. Complexes with octahedral, square pyramidal or tetrahedral geometries exhibit paramagnetism due to the presence of two unpaired electrons. In contrast, complexes with trigonal bipyramidal or square-planar geometries are diamagnetic, as they have no unpaired electrons.

The magnetic moments of the nickel (II) complex examined in this study were found to be diamagnetic. This observation strongly suggests that the nickel (II) complex possess a square planar geometry. This conclusion is further corroborated by evidence from electronic spectra.

Magnetically active cobalt (II) complexes are of two types

Two distinct electronic configurations are considered: i) three unpaired electrons and ii) a single unpaired electron. The former scenario is characteristic of high-spin octahedral and tetrahedral complexes, while the latter is observed in low-spin octahedral and square planar complexes.

Octahedral and tetrahedral cobalt (II) complexes typically exist in a high-spin state rather than a low-spin one. High-spin octahedral fields exhibit magnetic moments ranging from 4.7 to 5.2 B.M. These magnetic values result from both spin-only ($\mu = [4S (S+1)]1/2$) and spin plus orbital angular momentum ($\mu=[4S(S+1)+L(L+1)]1/2$). The actual magnetic moment depends on the extent of orbital angular momentum associated with the 4T1g ground state. In square planar complexes, L-S coupling increases the magnetic moment beyond the spin-only value. The Co(II) complex in this study exhibit magnetic moment 2.12 consistent with a square planar geometry. The analyzed Mn(II) complex exhibits a magnetic moment of 5.72, suggesting a high-spin octahedral geometry for the Mn(II) ion. The coordination sphere of the Mn(II) ion likely comprises four oxygen atoms (two from monodentate hydroxy groups of coordinated water molecules and two from Schiff base phenolic groups) and two nitrogen atoms from azomethine groups. However, in the absence of crystallographic data, this interpretation remains

speculative, relying solely on magnetic moment values and IR spectral data interpretations.

S.No	Complexes	μ_{eff} (BM)
1	$(TFPMP\text{-}SB3)_2$ Cu	1.72
2	$(TFPMP\text{-}SB3)_2$ Ni	0
3	$(TFPMP\text{-}SB3)_2$ Co	2.13
4	$(TFPMP\text{-}SB3)_2$ $(H_2O)_2$Mn	5.71

Table 1.5: Magnetic moment of (TFPMP-SB3) complexes

VII. ESR spectroscopy

ESR spectroscopy is a valuable technique for determining the coordination environment of Cu(II) ions. Cu(II) ions exhibit a diverse range of geometries, including tetrahedral, pentacoordinate, hexacoordinate, and various intermediate forms. The geometry of a Cu (II) complex significantly influences the energy levels of its d orbitals, consequently determining the ground state electronic configuration. Trigonal bipyramidal and compressed octahedral geometries typically result in a d_z^2 ground state. In contrast, square planar, elongated octahedral and square pyramidal geometries favor a $d_{x^2-y^2}$ ground state.

ESR spectroscopy can effectively differentiate between these ground states by analyzing the 'g' tensor values obtained from anisotropic spectra. These 'g' tensor values provide crucial information about the electronic environment of the unpaired electron in the Cu (II) ion, allowing for the determination of its specific ground state and, consequently, the geometry of the complex. This version maintains the original length while emphasizing the key aspects of ESR spectroscopy in determining Cu (II) ion environments.

The g value is a critical parameter in electron paramagnetic resonance (EPR) spectroscopy, analogous to the chemical shift in NMR spectroscopy. It signifies the response of a paramagnetic molecule to an external magnetic field. The g value is sensitive to changes in the molecule's electronic structure and provides a quantitative measure of its magnetic moment. For a free electron, the g value is approximately 2.0023. However, in metal complexes, the g value can deviate from this value, either increasing or decreasing.

Shifts in g values arise from spin-orbit coupling. ESR spectroscopy plays a crucial role in enhancing our understanding of copper's physiological significance within copper-containing compounds. The primary objective of ESR studies on copper (II) metal complexes is to elucidate information regarding the order of energy levels, metal-ligand bonding, and unpaired electron distribution. A considerable number of inorganic chemists currently utilize ESR spectroscopic measurements for investigating copper (II) complexes in the solid state.

In most copper (II) complexes, the ground state magnetism primarily arises from spin, with minimal orbital contributions. This is often referred to as "spin-only" magnetism. Since

copper(II) ions possess a $3d^9$ configuration with a single unpaired electron, the "effective" spin is equivalent to the actual spin of the free ion, S = 1/2. Zeeman splitting, characterized by 'g' factors, deviates from the free electron value of 2.0023 when spin-orbit coupling occurs between the ground and excited states. In this study, X-band ESR spectra of copper (II) complex was recorded at liquid nitrogen temperature (77 K) using a JES-FA200 ESR spectrometer (JEOL-Japan). Experimental parameters included a 9136.491 MHz microwave frequency, 0.99500 microwave power, and a 100.00 kHz modulation frequency. The corresponding spectra are presented in Fig .1.15. For square planar complexes, if the unpaired electron is present in the $d^{x^2-y^2}$ orbital then the trend follows the order as, $g_{\parallel}>g_{\perp}>g_e(2.0023)$, while if the unpaired electron is present in the d^{z^2} orbital then the trend follow the order as, $g_{\perp}>g_{\parallel}>g_e(2.0023)$. From the experimental values of copper (II) complex it is clear that $g_{\parallel}>g_{\perp}>g_e(2.0023)$. Which provides an evidence of localization of the unpaired electron in $dx^2–y^2$ orbital indicating square planar geometry of copper(II) complexes [24-28].The present ESR result for copper (II) complex exhibit $g_{\parallel}>g_{\perp}>g_e$ values below 2.3, indicative of a covalent character in the metal-ligand bond.

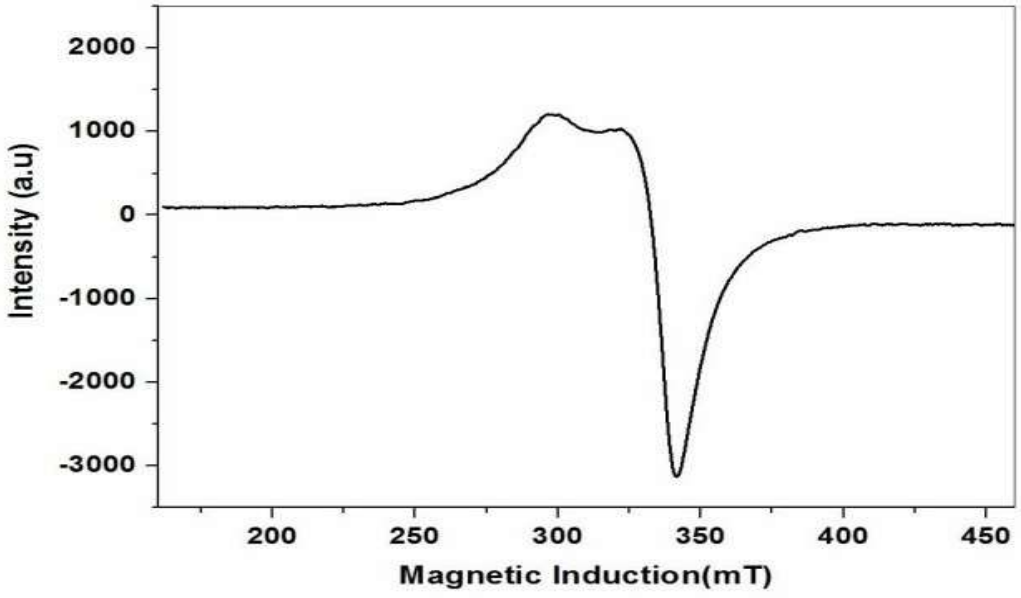

Fig .1.15.ESR Spectrum of $(TFPMP-SB3)_2Cu$

S.No	Complex	$g_{\parallel}$	$g_{\perp}$	G
1	$(TFPMP-SB3)_2$ Cu	2.12	2.07	1.61

Table 1.6: ESR Spectral Parameters for $(TFPMP-SB3)_2Cu$

Structure of the complexes of 2-(4-(trifluoromethyl) phenyl)imino)methyl)phenol (TFPMP-SB4)

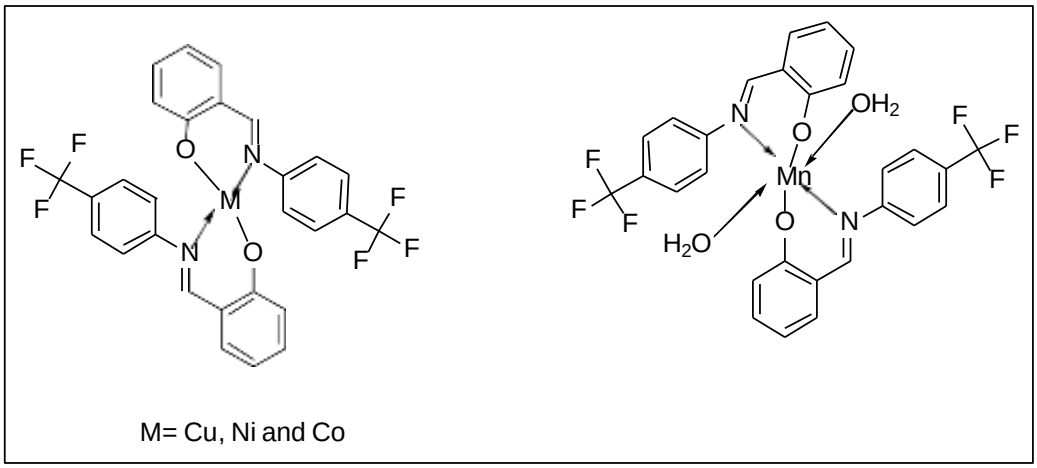

Biological activity:

In this study, the antifungal and antibacterial activities of synthesized Schiff bases and its metal complexes were screened. The agar cup method of diffusion was employed for biological screening against *Bacillus subtillis, Staphylococcus aureus, Escherichia coli, Klebsiella pneumonia, Aspergillus niger, Aspergillus foetidus, Candida albicans* and *Candida rogosa* utilizing nutrient broth as the culture medium.

a. Media Control: A control containing only sterilized medium is used to ensure the sterility of the medium itself. Growth in this control indicates improper sterilization, invalidating the results.
b. Organism Control: This control consists of sterilized medium inoculated with the test organism. Growth in this control confirms that the medium can support the growth of the organism. If no growth is observed, the medium may be inadequate for the organism's growth.
c. Solvent Control: This control includes sterilized medium, the solvent used to dissolve the test compound, and the test organism. Growth in this control indicates that the amount of solvent used does not inhibit the growth of the organism. If no growth is observed, the solvent may be inhibiting the organism's growth, rendering the test results invalid.

Test sample solutions were prepared at concentrations of 1 mg /1 mL. Subsequently, each solution was added to wells in agar plates inoculated with the desired bacterial and fungal strains. The plates were incubated at room temparature for 48 hours, followed by visual examination for the presence or absence of microbial growth. The findings of these studies for ligand (TFPMP-SB3) and its complexes are summarized in the tables below.

Anti-bacterial activity:

Antibacterial screening was performed against *Bacillus subtilis*, *Staphylococcus aureus*, *Escherichia coli*, and *Klebsiellapneumoniae* to evaluate the activity of a Schiff base and its metal complexes. Ampicillin was used as a positive control and demonstrated intermediate activity, producing inhibition zones of 30 mm against *E. coli*, 29 mm against *K. pneumoniae*, 25 mm against *B. subtilis*, and 28 mm against *S. aureus*.

Compound	Bacterial inhibition zone(mm)			
	Gram-negative bacteria		Gram-positive bacteria	
	E.col	*K.pneumonia*	*S.aureus*	*B.subtilis*
TFPMP-SB3	9	7	8	10
$(TFPMP\text{-}SB3)_2$ Cu	24	22	19	24
$(TFPMP\text{-}SB3)_2$ Ni	16	13	14	22
$(TFPMP\text{-}SB3)_2$ Co	18	16	17	15
$(TFPMP\text{-}SB3)_2(H_2O)_2Mn$	19	18	14	17
Ampicillin	30	29	25	28

Table 1.7: Antibacterial activity for ligand (TFPMP-SB3) and its complexes.

II. Antifungal activity of TFPMP-SB3 and its metal complexes:

The test compounds were subjected to screening against *Aspergillus niger*, *Aspergillus foetidus*, *Candida albicans and Candida rugosa* using nutrient broth as the culture medium by the agar cup diffusion method. Fluconazole was employed as a standard drug to compare the results.

Compound	Fungal inhibition zone(mm)			
	Aspergillus niger	*Aspergillus foetidus*	*Candida albicans*	*Candida rugosa*
TFPMP-SB3	10	09	07	08
$(TFPMP\text{-}SB3)_2$ Cu	22	17	17	21
$(TFPMP\text{-}SB3)_2$ Ni	14	11	12	22
$(TFPMP\text{-}SB3)_2$ Co	15	16	15	14
$(TFPMP\text{-}SB3)_2(H_2O)_2Mn$	13	12	14	16
Fluconazole	29	27	26	30

Table 1.8: Antifungal activity of (TFPMP-SB3) ligand and its metal complexes.

Conclusion:

Antimicrobial activity was assessed by measuring inhibition zone diameters after incubation. Concentrations of the ligand and its metal complexes demonstrated inhibitory effects against *E. coli*, *K. pneumoniae*, *S. aureus*, and *B. subtilis*, as evident from the data in the table. However, the complexes exhibited higher activity compared to the ligand. The results were compared against ampicillin, which showed intermediate activity. Based on these findings, the synthesized compounds exhibited weak antimicrobial activity against the studied microbes. The order of activity was observed as: Standard antibiotics > Complexes > Ligand and different concentrations of the ligand and its metal complexes demonstrated inhibitory effects against *Aspergillu sniger*, *Aspergillus foetidus*, *Candida albicans*, and *Candida rugosa*, as evident from the zone of inhibition data in the tables. However, the complexes exhibited higher activity compared to the ligand. The results were compared with a standard antifungal agent: Fluconazole, which showed intermediate activity. Based on these findings, the synthesized compounds exhibited weak antimicrobial activity against the studied microbes. The order of activity was observed as: Standard antifungal > Complexes > Ligand.

References:

1. Y. Marcus and I. Eliezer, Coord.Chem.Rev., 4 (1969) 273.
2. G.L. Eichorn (Ed), "Inorganic Biochemistry (Elsevier : Amsterdam), Vol. 1 & 2,(1973).
3. (a) H. Sigel, Angew.Chem.Int.Edit., 1, (1975) 394.
   (b) P.K. Bhattacharya, J. Scient.Ind.Res., 40, (1981) 382.
4. H. Siegel (Ed), "Metal ions in Biological Systems" (Marcell Dekker :New York), (1989) 1-23.
5. Y. Kinjo, L. Ji, N.A. Corfu and H. Siegel, Inorg.Chem., 31, (1992) 5588.
6. J.J.R. Frusto da Silva and R.J.P. Williams," The Biological Chemistry of the Elements" (Clandreon : Oxford), (1993).
7. CH. VenkataRamana Reddy and M.G. Ram Reddy J.Chem.Eng.Data., (1994).
8. L.A. Chrisey, G.H.S. Bonjar and S.M. Hecht, J.Am.Chem.Soc., 110 (1988) 644.
9. N.S.R.R. M.M.K. Rao and M.G. Ram Reddy, Biol. Met., 3 (1990) 19.
10. C.K. Rao, O. Babaiah, V.K. Reddy and T.S. Reddy, Talanta, 39 (1992) 1383.
11. A.E. Martell, "Metal ions in Biological Systems ("MarcellDekker:New York), vol.2, (1973) 5.
12. S.E. Sherman and S.J. Lippard, Chem.Rev., 87 (1987) 1153.
13. H. Schiff, Annalen, 31 (1864) 118.
14. P. Mishra, P.N. Gupta and A.K. Shakya, J.Ind. Chem Soc., 68 (1991) 618.
15. Y. Zhou, X. Ye, F. Xin, X. Xin, Transition Met. Chem. 24 (1999) 118.
16. D.X. West, A.K. El-Sawaf, G.A. Bain, Transit. Met.Chem. 23 (1998) 1.
17. R. Ramesh, S. Maheswaran, J. Inorg. Biochem.96 (2003) 457.
18. R.S. Joseyphus, C.J. Dhanaraj, M.S. Nair, Transit. Met.Chem. 31 (2006) 699.
19. R. Takjoo, R. Centore, A. Akbari, A. Mehdi, Polyhedron. 80 (2014) 243.
20. A.P. Mishra, S.K. Gautam, J. Indian.Chem. Soc. 81 (2004) 322.
21. S.A. Carabineiro, L.C. Silva, P.T. Gomes, C.J. Pereira, L.F. Veiros, I. Sofia, M. Pascu, D. Teresa, N. Sónia, R. T. Henriques, Inorg. Chem. 46 (2007) 6880.

22. Devi, J., Batra, N., and Malhotra, R. (2012). Spectrochim.ActaA Mol. Biomol. Spectrosc. 97, 397–405.
23. Keypour, H., Shayesteh, M., Rezaeivala, M., Chalabian, F., and Valencia, L. (2013). Spectrochim.ActaA Mol. Biomol. Spectrosc.101, 59–66 (2013).
24. E. Erdem, E.Y. Sari, R. Kilinçarslan, N. Kabay, Transition Met.Chem. 34 (2009) 167.
25. L.J. Bellamy, The Infrared Spectra of Complex Molecules, second ed., Chapmann and Hall, London, 1980.
26. P.P. Dholayika, M.N. Patel, Synth. React. Inorg.Met-Org. Nano-Chem. 34 (2004) 383.
27. F.A. Cotton, G. Wilkinson, Advanced Inorganic Chemistry, third ed., InterscicencePublisher, New York, 1972.
28. A.B.P. Lever, Inorganic Electronic Spectroscopy, second ed., Elsevier, Amsterdam,1984.151